

Multiple Production of $MSSM$ Neutral Higgs Bosons at High-Energy e^+e^- Colliders

A. DJOUADI^{1,2*}, H.E. HABER³, AND P.M. ZERWAS²

¹ Institute für Theoretische Physik, Universität Karlsruhe,
D-76128 Karlsruhe, FRG.

² Deutsches Elektronen-Synchrotron DESY, D-22603 Hamburg, FRG.

³ Santa Cruz Institute for Particle Physics, University of California,
Santa Cruz, CA 95064, USA.

Abstract

The cross sections for the multiple production of the lightest neutral Higgs boson at high-energy e^+e^- colliders are presented in the framework of the Minimal Supersymmetric extension of the Standard Model ($MSSM$). We consider production through Higgs-strahlung, associated production of the scalar and the pseudoscalar bosons, and the fusion mechanisms for which we use the effective longitudinal vector-boson approximation. These cross sections allow one to determine trilinear Higgs couplings λ_{Hhh} and λ_{hhh} , which are theoretically determined by the Higgs potential.

*Supported by Deutsche Forschungsgemeinschaft DFG (Bonn).

1. Introduction

The only unknown parameter in the Standard Model (\mathcal{SM}) is the quartic coupling of the Higgs field in the potential, which determines the value of the Higgs mass. If the Higgs mass is known, the potential is uniquely fixed. Since the form of the Higgs potential is crucial for the mechanism of spontaneous symmetry breaking, *i.e.* for the Higgs mechanism *per se*, it will be very important to measure the coefficients in the potential once Higgs particles have been discovered.

If the mass of the scalar particle is less than about 150 GeV, it very likely belongs to the quintet of Higgs bosons, h, H, A, H^\pm predicted in the two-doublet Higgs sector of supersymmetric theories [1] [h and H are the light and heavy CP-even Higgs bosons, A is the CP-odd (pseudoscalar) Higgs boson, and H^\pm is the charged Higgs pair]. The potential of the two doublet Higgs fields, even in the Minimal Supersymmetric Standard Model (\mathcal{MSSM}), is much more involved than in the Standard Model [2]. If CP is conserved by the potential, the most general two-doublet model contains three mass parameters and seven real self-couplings. In the \mathcal{MSSM} , the potential automatically conserves CP; in addition, supersymmetry fixes all the Higgs self-couplings in terms of gauge couplings. The remaining three free mass parameters can be traded in for the two vacuum expectation values (VEV's) of the neutral Higgs fields and one of the physical Higgs masses. The sum of the squares of the VEV's is fixed by the W mass, while the ratio of VEV's is a free parameter of the model called $\tan\beta$. It is theoretically convenient to choose the free parameters of the \mathcal{MSSM} Higgs sector to be $\tan\beta$ and M_A , the mass of the CP-odd Higgs boson A . The other Higgs masses and the mixing angle α of the CP-even neutral sector are then determined. Moreover, since all coefficients in the Higgs potential are also determined, the trilinear and quartic self-couplings of the physical Higgs particles can be predicted theoretically. By measuring these couplings, the Higgs potential can be reconstructed – an experimental *prima facie* task to establish the Higgs mechanism as the basic mechanism for generating the masses of the fundamental particles.

The endeavor of measuring all Higgs self-couplings in the \mathcal{MSSM} is a daunting task. We will therefore discuss a first step by analyzing theoretically the production of two light Higgs particles of the \mathcal{MSSM} . These processes may be studied at the proton collider LHC [3] and at a high-energy e^+e^- linear collider. In this paper we will focus on the e^+e^- accelerators that are expected to operate in the first phase at an energy of 500 GeV with a luminosity of about $\int \mathcal{L} = 20 \text{ fb}^{-1}$, and in a second phase at an energy of about 1.5 TeV with a luminosity of order $\int \mathcal{L} = 200 \text{ fb}^{-1}$ *per annum* [4]. They will allow us to eventually study the couplings λ_{Hhh} and λ_{hhh} . The measurement of the coupling λ_{hAA} will be very difficult.

Multiple light Higgs bosons h can [in principle] be generated in the \mathcal{MSSM} by four mechanisms¹:

¹The production of two light Higgs bosons, $e^+e^- \rightarrow hh$, through loop diagrams does not involve any trilinear Higgs coupling; the production rates are rather small [5].

(i) Decay of the heavy CP-even neutral Higgs boson, produced either by H -strahlung and associated AH pair production, or in the WW fusion mechanisms, Fig. 1a,

$$\left. \begin{array}{l} e^+e^- \rightarrow ZH, AH \\ e^+e^- \rightarrow \nu_e \bar{\nu}_e H \end{array} \right\} \quad H \rightarrow hh \quad (1)$$

Associated production $e^+e^- \rightarrow hA$ followed by $A \rightarrow hZ$ decays leads to hhZ background final states.

(ii) Double Higgs-strahlung in the continuum, with a final state Z boson, Fig. 1b,

$$e^+e^- \rightarrow Z^* \rightarrow hhZ \quad (2)$$

(iii) Associated production with the pseudoscalar A in the continuum, Fig. 1c,

$$e^+e^- \rightarrow Z^* \rightarrow hhA \quad (3)$$

(iv) Non-resonant $WW(ZZ)$ fusion in the continuum, Fig. 1d,

$$e^+e^- \rightarrow \bar{\nu}_e \nu_e W^* W^* \rightarrow \bar{\nu}_e \nu_e hh \quad (4)$$

The cross sections for ZZ fusion in (1) and (4) are suppressed by an order of magnitude. The largest cross sections can be anticipated for the processes (1), where heavy on-shell H Higgs bosons decay into pairs of the light Higgs bosons. [Cross sections of similar size are expected for the backgrounds involving the pseudoscalar Higgs bosons.] We have derived the cross sections for the four processes analytically; the fusion process has been treated in the equivalent particle approximation for longitudinal vector bosons.

We will carry out the analysis in the \mathcal{MSSM} for the value $\tan\beta = 1.5$. [A summary will be given in the last section for all values of $\tan\beta$]. In the present exploratory study, squark mixing will be neglected, *i.e.* the supersymmetric Higgs mass parameter μ and the parameter A_t in the soft symmetry breaking interaction will be set to zero, and the radiative corrections will be included in the leading m_t^4 one-loop approximation parameterized by [6]

$$\epsilon = \frac{3G_F}{\sqrt{2}\pi^2} \frac{m_t^4}{\sin^2\beta} \log \left(1 + \frac{M_S^2}{m_t^2} \right) \quad (5)$$

with the common squark mass fixed to $M_S = 1$ TeV. In terms of $\tan\beta$ and M_A , the trilinear Higgs couplings relevant for our analysis are given in this approximation by

$$\begin{aligned} \lambda_{hhh} &= 3 \cos 2\alpha \sin(\beta + \alpha) + 3 \frac{\epsilon}{M_Z^2} \frac{\cos^3 \alpha}{\sin \beta} \\ \lambda_{Hhh} &= 2 \sin 2\alpha \sin(\beta + \alpha) - \cos 2\alpha \cos(\beta + \alpha) + 3 \frac{\epsilon}{M_Z^2} \frac{\sin \alpha}{\sin \beta} \cos^2 \alpha \end{aligned} \quad (6)$$

In addition, the coupling

$$\lambda_{hAA} = \cos 2\beta \sin(\beta + \alpha) + \frac{\epsilon}{M_Z^2} \frac{\cos \alpha}{\sin \beta} \cos^2 \beta \quad (7)$$

will be needed even though it turned out – *a posteriori* – that it cannot be measured using the experimental methods discussed in this note². As usual, these couplings are defined in units of $(2\sqrt{2}G_F)^{1/2}M_Z^2$; the h, H, H^\pm masses and the mixing angle α can be expressed in terms of M_A and $\tan\beta$ [see e.g. Ref. [8] for a recent discussion].

In the decoupling limit [9] for large A, H and H^\pm masses, the lightest Higgs particle becomes \mathcal{SM} -like and the trilinear hhh coupling approaches the \mathcal{SM} value $\lambda_{hhh} \rightarrow M_h^2/M_Z^2$. In this limit, only the first three diagrams of Fig. 1b and 1d contribute and the cross-sections for the processes $e^+e^- \rightarrow hhZ$ and $WW \rightarrow hh$ approach the corresponding cross sections of the \mathcal{SM} [10, 11].

2. H Production and hh Decays

If kinematically allowed, the most copious source of multiple h final states are cascade decays $H \rightarrow hh$, with H produced either by Higgs-strahlung or associated pair production [1],

$$\sigma(e^+e^- \rightarrow ZH) = \frac{G_F^2 M_Z^4}{96\pi s} (v_e^2 + a_e^2) \cos^2(\beta - \alpha) \frac{\lambda_Z^{1/2} [\lambda_Z + 12M_Z^2/s]}{(1 - M_Z^2/s)^2} \quad (8)$$

$$\sigma(e^+e^- \rightarrow AH) = \frac{G_F^2 M_Z^4}{96\pi s} (v_e^2 + a_e^2) \sin^2(\beta - \alpha) \frac{\lambda_A^{3/2}}{(1 - M_Z^2/s)^2} \quad (9)$$

The Z couplings to electrons are given by $a_e = -1, v_e = -1 + 4\sin^2\theta_W$ and λ_j is the usual two-body phase space function $\lambda_j = (1 - M_j^2/s - M_H^2/s)^2 - 4M_j^2 M_H^2/s^2$. The cross sections (8) and (9) are shown in Fig. 2 for the total e^+e^- energies $\sqrt{s} = 500$ GeV and 1.5 TeV as a function of the Higgs mass M_H for a small value of $\tan\beta = 1.5$ where the H cascade decays are significant over a large mass range. As a consequence of the decoupling theorem, associated AH production is dominant for large Higgs masses.

The trilinear Hhh coupling can be measured in the decay process $H \rightarrow hh$

$$\Gamma(H \rightarrow hh) = \frac{G_F \lambda_{Hhh}^2}{16\sqrt{2}\pi} \frac{M_Z^4}{M_H} \left(1 - \frac{4M_h^2}{M_H^2}\right)^{1/2} \quad (10)$$

if the branching ratio is neither too small nor too close to unity. This is indeed the case, as shown in Fig. 3a, for H masses between 180 and 350 GeV and small to moderate $\tan\beta$ values. The other important decay modes are WW^*/ZZ^* decays. Since the H couplings

²For small masses the decay $h \rightarrow AA$ could have provided an experimental opportunity to measure this coupling. However, for $\tan\beta > 1$, this area of the $MSSM$ parameter space has been excluded by LEP [7].

to the gauge bosons can be measured through the production cross sections of the fusion and Higgs-strahlung processes, the branching ratio $\text{BR}(H \rightarrow hh)$ can be exploited to measure the coupling λ_{Hhh} .

The ZH final state gives rise to resonant two-Higgs $[hh]$ final states. The AH final state typically yields three Higgs $h[hh]$ final states since the channel $A \rightarrow hZ$ is the dominant decay mode in most of the mass range we consider. This is shown in Fig. 3b where the branching ratios of the pseudoscalar A are displayed for $\text{tg}\beta = 1.5$.

Another type of two-Higgs hh final states is generated in the chain $e^+e^- \rightarrow Ah \rightarrow [Zh]h$, which does not involve any of the Higgs self-couplings. However, in this case, the two h bosons do not resonate while $[Zh]$ does, so that the topology of these background events is very different from the signal events. The size of the $e^+e^- \rightarrow hA$ background cross section is shown in Fig. 2 together with the signal cross sections; for sufficiently large M_A , it becomes small, in line with the decoupling theorem [9].

A second large signal cross section is provided by the WW fusion mechanism. [Since the NC couplings are smaller compared to the CC couplings, the cross section for the ZZ fusion processes in (1) and (4) is $\sim 16 \cos^4 \theta_W$, *i.e.* one order of magnitude smaller than for WW fusion.] In the effective longitudinal W approximation [12] one obtains

$$\sigma(e^+e^- \rightarrow H\bar{\nu}_e\nu_e) = \frac{G_F^3 M_W^4}{4\sqrt{2}\pi} \left[\left(1 + \frac{M_H^2}{s}\right) \log \frac{s}{M_H^2} - 2 \left(1 - \frac{M_H^2}{s}\right) \right] \cos^2(\beta - \alpha) \quad (11)$$

The magnitude of the cross section³ $e^+e^- \rightarrow H\nu_e\bar{\nu}_e$ is also shown in Fig. 2 for the two energies $\sqrt{s} = 500$ GeV and 1.5 TeV as a function of the Higgs mass M_H and for $\text{tg}\beta = 1.5$. The signals in $e^+e^- \rightarrow [hh] + \text{missing energy}$ are very clear, competing only with H -strahlung and subsequent neutrino decays of the Z boson. Since the lightest Higgs boson will decay mainly into $b\bar{b}$ pairs, the final states will predominantly include four and six b quarks.

At $\sqrt{s} = 500$ GeV, about 500 signal events are predicted in the mass range of $M_H \sim 200$ GeV for an integrated luminosity of $\int \mathcal{L} = 20 \text{ fb}^{-1}$ *per annum*; and at $\sqrt{s} = 1.5$ TeV, about 8,000 to 1,000 signal events for the prospective integrated luminosity of $\int \mathcal{L} = 200 \text{ fb}^{-1}$ *per annum* in the interesting mass range between 180 and 350 GeV. Note that for both energies, the Ah background cross section is significantly smaller.

3. Non-Resonant Double hh Production

The double Higgs-strahlung $e^+e^- \rightarrow Zh$, the triple Higgs production process $e^+e^- \rightarrow Ahh$ and the WW fusion mechanism $e^+e^- \rightarrow \nu_e\bar{\nu}_e hh$ outside the resonant $H \rightarrow hh$ range are disfavored by an additional power of the electroweak coupling compared to the resonance processes. Nevertheless, these processes must be analyzed carefully in order to measure the value of the hhh coupling.

³In the effective W approximation, the cross section may be overestimated by as much as a factor of 2 for small masses and/or small c.m. energies. Therefore we display the exact cross sections [13] in Fig.2.

3.1 $e^+e^- \rightarrow Zh h$

The double differential cross section of the process $e^+e^- \rightarrow hhZ$, Fig. 1b, is given by

$$\frac{d\sigma(e^+e^- \rightarrow hhZ)}{dx_1 dx_2} = \frac{G_F^3 M_Z^6}{384\sqrt{2}\pi^3 s} (a_e^2 + v_e^2) \frac{\mathcal{A}}{(1 - \mu_Z)^2} \quad (12)$$

The couplings have been defined in the previous section. $x_{1,2} = 2E_{1,2}/\sqrt{s}$ are the scaled energies of the Higgs particles, $x_3 = 2 - x_1 - x_2$ is the scaled energy of the Z boson; $y_k = 1 - x_k$. The scaled masses squared are denoted by $\mu_i = M_i^2/s$. In terms of these variables, the coefficient \mathcal{A} in the cross section may be written as:

$$\begin{aligned} \mathcal{A} = & \left\{ \frac{a^2}{2} f_0 + \frac{\sin^4(\beta - \alpha)}{4\mu_Z^2(y_1 + \mu_h - \mu_Z)} \left[\frac{f_1}{y_1 + \mu_h - \mu_Z} + \frac{f_2}{y_2 + \mu_h - \mu_Z} \right] + \frac{\cos^4(\beta - \alpha)}{4\mu_Z^2(y_1 + \mu_h - \mu_A)} \right. \\ & \times \left[\frac{f_3}{y_1 + \mu_h - \mu_A} + \frac{f_4}{y_2 + \mu_h - \mu_A} \right] + \frac{a}{\mu_Z} \left[\frac{\sin^2(\beta - \alpha)f_5}{y_1 + \mu_h - \mu_Z} + \frac{\cos^2(\beta - \alpha)f_6}{y_1 + \mu_h - \mu_A} \right] \\ & \left. + \frac{\sin^2 2(\beta - \alpha)}{8\mu_Z^2(y_1 + \mu_h - \mu_Z)} \left[\frac{f_7}{y_1 + \mu_h - \mu_Z} + \frac{f_8}{y_2 + \mu_h - \mu_Z} \right] \right\} + \{y_1 \leftrightarrow y_2\} \quad (13) \end{aligned}$$

with

$$a = \frac{1}{2} \left[\frac{\sin(\beta - \alpha)\lambda_{hhh}}{y_3 + \mu_Z - \mu_h} + \frac{\cos(\beta - \alpha)\lambda_{Hhh}}{y_3 + \mu_Z - \mu_H} \right] + \frac{\sin^2(\beta - \alpha)}{y_1 + \mu_h - \mu_Z} + \frac{\sin^2(\beta - \alpha)}{y_2 + \mu_h - \mu_Z} + \frac{1}{2\mu_Z} \quad (14)$$

[omitting the small decay widths of the Higgs bosons]. Only the coefficient a includes the Higgs self-couplings λ_{Hhh} and λ_{hhh} . Introducing the notation $y_0 = (y_1 - y_2)/2$, the coefficients f_i which do not involve any Higgs couplings, are defined by

$$\begin{aligned} f_0 &= (y_1 + y_2)^2 - 4\mu_Z(1 - 3\mu_Z) \\ f_1 &= [(1 + y_1)^2 - 4\mu_Z(y_1 + \mu_h)] [y_1^2 + \mu_Z^2 - 2\mu_Z(y_1 + 2\mu_h)] \\ f_2 &= [2\mu_Z(\mu_Z - 2\mu_h + 1) - (1 + y_1)(1 + y_2)] [\mu_Z(\mu_Z - y_1 - y_2 - 4\mu_h + 2) - y_1 y_2] \\ f_3 &= [y_0^2 + \mu_Z(1 - y_1 - y_2 + \mu_Z - 4\mu_h)] [1 + y_1 + y_2 + y_0^2 + \mu_Z(\mu_Z - 4\mu_h - 2y_1)] \\ f_4 &= [y_0^2 + \mu_Z(1 - y_1 - y_2 + \mu_Z - 4\mu_h)] [y_0^2 - 1 + \mu_Z(\mu_Z - y_1 - y_2 - 4\mu_h + 2)] \\ f_5 &= 2\mu_Z^3 - 4\mu_Z^2(y_1 + 2\mu_h) + \mu_Z[(1 + y_1)(3y_1 - y_2) + 2] - y_1^2(1 + y_1 + y_2) - y_1 y_2 \\ f_6 &= 2\mu_Z^3 - \mu_Z^2(y_2 + 3y_1 + 8\mu_h - 2) + 2\mu_Z y_0(1 + y_1 + y_0) + 2y_1 y_0 - y_0^2(y_1 + y_2 - 2) \\ f_7 &= [\mu_Z(4\mu_h - \mu_Z - 1 + 2y_1 - y_0) - y_1 y_0] [\mu_Z(4\mu_h - \mu_Z - 1 + 3y_1) - (1 + y_0)(1 + y_1)] \\ f_8 &= [\mu_Z(4\mu_h - \mu_Z - 1 + 2y_1 - y_0) - y_1 y_0] [\mu_Z(4\mu_h - \mu_Z - 2 + y_1) + (1 - y_0)(1 + y_1)] \end{aligned} \quad (15)$$

In the decoupling limit, the cross section is reduced to the \mathcal{SM} cross section for which

$$\mathcal{A} = \frac{a^2}{2} f_0 + \frac{1}{4\mu_Z^2(y_1 + \mu_h - \mu_Z)} \left[\frac{f_1}{y_1 + \mu_h - \mu_Z} + \frac{f_2}{y_2 + \mu_h - \mu_Z} + 4a\mu_Z f_5 \right] + \{y_1 \leftrightarrow y_2\}$$

with the f_i 's as given above, and

$$a = \frac{1}{2} \frac{\lambda_{hhh}}{y_3 + \mu_Z - \mu_h} + \frac{1}{y_1 + \mu_h - \mu_Z} + \frac{1}{y_2 + \mu_h - \mu_Z} + \frac{1}{2\mu_Z}$$

The cross section $\sigma(e^+e^- \rightarrow hhZ)$ is shown for $\sqrt{s} = 500$ GeV at $\tan\beta = 1.5$ as a function of the Higgs mass M_h in Fig. 4a. For small masses, the cross section is built up almost exclusively by $H \rightarrow hh$ decays [dashed curve], except close to the point where the λ_{Hhh} coupling accidentally vanishes (cf. Ref.[8]) and for masses around ~ 90 GeV where additional contributions come from the decay $A \rightarrow hZ$ [this range of M_h corresponds to M_A values where $\text{BR}(A \rightarrow hZ)$ is large; c.f. Fig.3]. For intermediate masses, the resonance contribution is reduced and, in particular above 90 GeV where the decoupling limit is approached, the continuum hh production becomes dominant, falling finally down to the cross section for double Higgs production in the Standard Model [dashed line]. After subtracting the $H \rightarrow hh$ decays [which of course is very difficult], the continuum cross section is about 0.5 fb, and is of the same order as the \mathcal{SM} cross section at $\sqrt{s} = 500$ GeV. Very high luminosity is therefore needed to measure the trilinear hhh coupling. At higher energies, since the cross section for double Higgs-strahlung scales like $1/s$, the rates are correspondingly smaller, c.f. Fig.4b.

Prospects are similar for large $\tan\beta$ values. The cascade decay $H \rightarrow hh$ is restricted to a small M_h range of less than 70 GeV, with a production cross section of ~ 20 fb at $\sqrt{s} = 500$ GeV and ~ 3 fb at 1.5 TeV. The continuum cross sections are of the order of 0.1 fb at both energies, so that very high luminosities will be needed to measure the continuum cross sections in this case if the background problems can be mastered at all.

We have repeated the analysis for the continuum process $e^+e^- \rightarrow Ahh$ (cf. Fig.1c). However, it turned out that the cross section is built up almost exclusively by resonant $AH \rightarrow Ahh$ final states, with a very small continuum contribution, so that the measurement of the coupling λ_{hAA} is extremely difficult in this process.

3.2 $W_L W_L \rightarrow hh$

In the effective longitudinal W approximation⁴, the total cross section for the subprocess $W_L W_L \rightarrow hh$, Fig. 1d, is given by

$$\begin{aligned} \hat{\sigma}_{LL} = & \frac{G_F^2 \hat{s}}{64\pi} \frac{\beta_h}{\beta_W} \left\{ (1 + \beta_W^2)^2 \left[\frac{\mu_Z \sin(\beta - \alpha)}{1 - \mu_h} \lambda_{hhh} + \frac{\mu_Z \cos(\beta - \alpha)}{1 - \mu_H} \lambda_{Hhh} + 1 \right]^2 \right. \\ & + \frac{\beta_W^2}{\beta_W \beta_h} \left[\frac{\mu_Z \sin(\beta - \alpha)}{1 - \mu_h} \lambda_{hhh} + \frac{\mu_Z \cos(\beta - \alpha)}{1 - \mu_H} \lambda_{Hhh} + 1 \right] [\sin^2(\beta - \alpha) g_1 \\ & + \cos^2(\beta - \alpha) g_2] + \frac{1}{\beta_W^2 \beta_h^2} [\sin^4(\beta - \alpha) g_3 + \cos^4(\beta - \alpha) g_4 + \sin^2 2(\beta - \alpha) g_5] \left. \right\} \end{aligned} \quad (16)$$

⁴For qualifying comments see footnote 3.

with

$$\begin{aligned}
g_1 &= 2[(\beta_W - x_W \beta_h)^2 + 1 - \beta_W^4]l_W - 4\beta_h(2\beta_W - x_W \beta_h) \\
g_2 &= 2(x_C \beta_h - \beta_W)^2 l_C + 4\beta_h(x_C \beta_h - 2\beta_W) \\
g_3 &= \beta_h[\beta_h x_W(3\beta_h^2 x_W^2 + 14\beta_W^2 + 2 - 2\beta_W^4) - 4\beta_W(3\beta_h^2 x_W^2 + \beta_W^2 + 1 - \beta_W^4)][l_W + x_W y_W] \\
&\quad - [\beta_W^4 + (1 - \beta_W^4)(1 + 2\beta_W^2 - \beta_W^4)][l_W/x_W - y_W] - 2\beta_h^2 y_W(2\beta_W - \beta_h x_W)^2 \\
g_4 &= \beta_h[\beta_h x_C(3\beta_h^2 x_C^2 + 14\beta_W^2) - 4\beta_W(3\beta_h^2 x_C^2 + \beta_W^2)][l_C + x_C y_C] \\
&\quad - \beta_W^4[l_C/x_C - y_C] - 2y_C \beta_h^2(2\beta_W - \beta_h x_C)^2 \\
g_5 &= \frac{\beta_h \beta_W l_W}{x_W^2 - x_C^2} [2x_W(2x_W^2 \beta_h \beta_W - x_C x_W^2 \beta_h^2 - x_C \beta_W^2) - 2x_W^2(\beta_h^2 x_W^2 + \beta_W^2 + 1 - \beta_W^4) \\
&\quad + \frac{x_C}{\beta_W \beta_h} ((\beta_h^2 x_W^2 + \beta_W^2)(1 - \beta_W^4) + (\beta_h^2 x_W^2 + \beta_W^2)^2)] - 4\beta_h^3 \beta_W(x_W + x_C) \\
&\quad + \frac{\beta_h \beta_W l_C}{x_C^2 - x_W^2} [4x_C^3 \beta_h \beta_W - 2x_C x_W(\beta_h^2 x_C^2 + \beta_W^2 + 1 - \beta_W^4) - 2x_C^2(\beta_h^2 x_C^2 + \beta_W^2) \\
&\quad + \frac{x_W}{\beta_W \beta_h} ((\beta_W^2 + \beta_h^2 x_C^2)(1 - \beta_W^4) + (\beta_h^2 x_C^2 + \beta_W^2)^2)] + 2\beta_h^2(x_C x_W \beta_h^2 + 4\beta_W^2) \quad (17)
\end{aligned}$$

The scaling variables are defined in the same way as before. $\hat{s}^{1/2}$ is the c.m. energy of the subprocess, $\beta_W = (1 - 4M_W^2/\hat{s})^{1/2}$ and $\beta_h = (1 - 4M_h^2/\hat{s})^{1/2}$ are the velocities of the W and h bosons, and

$$\begin{aligned}
x_W &= (1 - 2\mu_h)/(\beta_W \beta_h) \quad , \quad x_C = (1 - 2\mu_h + 2\mu_{H^\pm} - 2\mu_W)/(\beta_W \beta_h) \\
l_i &= \log(x_i - 1)/(x_i + 1) \quad , \quad y_i = 2/(x_i^2 - 1) \quad (18)
\end{aligned}$$

The value of the charged Higgs boson mass M_{H^\pm} in the $H^\pm t$ -channel exchange diagram of Fig.1d is given by $M_{H^\pm}^2 = M_A^2 + M_W^2$.

In the decoupling limit, the cross section reduces again to the \mathcal{SM} cross section which in terms of g_1 and g_2 , defined above, is given by:

$$\hat{\sigma}_{LL} = \frac{G_F^2 \hat{s}}{64\pi} \frac{\beta_h}{\beta_W} \left\{ (1 + \beta_W^2)^2 \left[\frac{\mu_Z \lambda_{hhh}}{1 - \mu_h} + 1 \right]^2 + \frac{1 + \beta_W^2}{\beta_W \beta_h} \left[\frac{\mu_Z \lambda_{hhh}}{1 - h_1} + 1 \right] g_1 + \frac{g_3}{\beta_W^2 \beta_h^2} \right\} \quad (19)$$

After folding $\hat{\sigma}_{LL}$ with the longitudinal $W_L W_L$ luminosity [12], one obtains the total cross section $\sigma(e^+ e^- \rightarrow \nu_e \bar{\nu}_e h h)$ shown in Fig. 4b as a function of the light Higgs mass M_h for $\text{tg}\beta = 1.5$ at $\sqrt{s} = 1.5$ TeV. It is significantly larger than for double Higgs-strahlung in the continuum. Again, for very light Higgs masses, most of the events are $H \rightarrow hh$ decays [dashed line]. The continuum hh production is of the same size as pair production of \mathcal{SM} Higgs bosons [dotted line] which, as anticipated, is being approached near the upper limit of the h mass in the decoupling limit. The size of the continuum hh fusion cross section renders this channel more promising than double Higgs-strahlung for the measurement of the trilinear hhh coupling.

For large $\text{tg}\beta$ values, strong destructive interference effects reduce the cross section in the continuum to very small values, of order 10^{-2} fb, before the \mathcal{SM} cross section is

reached again in the decoupling limit. As before, the hh final state is almost exclusively built up by the resonance $H \rightarrow hh$ decays.

4. Summa

It is convenient to summarize our results by presenting Fig.5, which displays the areas of the $[M_A, \text{tg}\beta]$ plane in which λ_{Hhh} [solid lines, 135° hatching] and λ_{hhh} [dashed lines, 45° hatching] could eventually be accessible by experiment. The size of these areas is based on purely theoretical cuts so that they are expected to shrink if background processes and detector effects are taken into account.

(i) In the case of $H \rightarrow hh$, we require a lower limit of the cross section $\sigma(H) \times \text{BR}(H \rightarrow hh) > 0.5$ fb and at the same time for the decay branching ratio $0.1 < \text{BR}(H \rightarrow hh) < 0.9$, as discussed earlier. Based on these definitions, λ_{Hhh} may become accessible in two disconnected regions denoted by I and II [135° hatched] in Fig.5. For low $\text{tg}\beta$, the left boundary of Region I is set by LEP1 data. The gap between Regions I and II is a result of the nearly vanishing λ_{Hhh} coupling in this strip. The right boundary of Region II is due to the overwhelming $t\bar{t}$ decay mode for heavy H masses, as well as due to the small H production cross section. For moderate values of $\text{tg}\beta$, the left boundary of Region I is defined by $\text{BR}(H \rightarrow hh) > 0.9$. In the area between Regions I and II, H cannot decay into two h bosons, *i.e.* $M_H < 2M_h$. For large $\text{tg}\beta \gtrsim 10$, $\text{BR}[H \rightarrow hh(AA)]$ is either too large or too small, except in a very small strip, $M_A \simeq 65$ GeV, towards the top of Region I. [Note that h and A are nearly mass-degenerate in this area.]

(ii) The dashed line in Fig.5 describes the left boundary of the area [45° hatched] in which λ_{hhh} may become accessible; it is defined by the requirement that the continuum $W_L W_L \rightarrow hh$ cross section, σ_{cont} , is larger than 0.5 fb. Note that the resonant $H \rightarrow hh$ events in Region II must be subtracted in order to extract the λ_{hhh} coupling.

In conclusion, we have derived the cross sections for the double production of the lightest neutral Higgs boson in the \mathcal{MSSM} at e^+e^- colliders: in the Higgs-strahlung process $e^+e^- \rightarrow Zhh$, [in the triple Higgs production process $e^+e^- \rightarrow Ahh$], and in the WW fusion mechanism. These cross sections are large for resonant $H \rightarrow hh$ decays so that the measurement of the triple Higgs coupling λ_{Hhh} is expected to be fairly easy for $H \rightarrow hh$ decays in the M_H mass range between 150 and 350 GeV for small $\text{tg}\beta$ values. The continuum processes must be exploited to measure the triple Higgs coupling λ_{hhh} . These continuum cross sections, which are of the same size as in the \mathcal{SM} , are rather small so that high luminosities are needed for the measurement of the triple Higgs coupling λ_{hhh} .

Acknowledgements:

Discussions with G. Moulton and technical help by T. Plehn are gratefully acknowledged. A.D. thanks the Theory Group for the warm hospitality extended to him at DESY, and H.E.H. acknowledges the partial support of the U.S. Department of Energy.

References

- [1] For reviews on the Higgs sector in the SM and $MSSM$, see J.F. Gunion, H.E. Haber, G. Kane and S. Dawson, *The Higgs Hunter's Guide*, Addison–Wesley 1990; A. Djouadi, Int. J. Mod. Phys A10 (1995) 1.
- [2] J.F. Gunion and H.E. Haber, Nucl. Phys. B272 (1986) 1; B278 (1986) 449.
- [3] T. Plehn, M. Spira and P. M. Zerwas, DESY 95–215 and Z. Phys. C (in press).
- [4] See *e.g.* P.M. Zerwas, Proceedings, *Les Rencontres de Physique de la Vallée d'Aoste*, La Thuile 1994 and DESY 94–001.
- [5] K. Gaemers and F. Hoogeveen, Z. Phys. C26 (1984) 249; A. Djouadi, V. Driesen and C. Jünger, Report KA–TP–02–96.
- [6] H.E. Haber and R. Hempfling, Phys. Rev. Lett. 66 (1991) 1815; Y. Okada, M. Yamaguchi and T. Yanagida, Prog. Theor. Phys. 85 (1991) 1; J. Ellis, G. Ridolfi and F. Zwirner, Phys. Lett. 257B (1991) 83.
- [7] J.-F. Grivaz, Proceedings, *Int. Conference on High-Energy Physics*, Brussels 1995.
- [8] A. Djouadi, J. Kalinowski and P. M. Zerwas, DESY 95–211 (hep-ph 9511342) and Z. Phys. C (in press).
- [9] H.E. Haber, CERN-TH/95-109 and SCIPP-95/15, Proceedings, *Conference on Physics Beyond the Standard Model IV*, Lake Tahoe CA 1994; and *Perspectives for Electroweak Interactions in e^+e^- Collisions*, Ringberg Castle, Tegernsee 1995.
- [10] G. Gounaris, D. Schildknecht and F. Renard, Phys. Lett. B83 (1979) 191 and (E) 89B (1980) 437.
- [11] V. Barger and T. Han, Mod. Phys. Lett. A5 (1990) 667; V. Barger, T. Han and R.J. Phillips, Phys. Rev. D38 (1988) 2766; J. F. Gunion et al., Phys. Rev. D38 (1988) 3444; D. Dicus, K. Kallianpur and S. Willenbrock, Phys. Lett. B200 (1988) 187; K. Kallianpur, Phys. Lett. B215 (1988) 392; A. Abbasabadi, W. Repko, D. Dicus and R. Vega, Phys. Rev. D38 (1988) 2770; V. Ilyin, A. Pukhov, Y. Kurihara, Y. Shimitzu and T. Kaneko, KEK CP–030; F. Boudjema and E. Chopin, ENSLAPP–A534/95.
- [12] R.N. Cahn and S. Dawson, Phys. Lett. B136 (1984) 196; S. Dawson, Nucl. Phys. B249 (1984) 42; S. Chanowitz and M.K. Gaillard, Phys. Lett. B142 (1984) 85; I. Kuss and H. Spiesberger, Report BI–TP–95/25.
- [13] A. Djouadi, D. Haidt, B. Kniehl, B. Mele and P.M. Zerwas, Proceedings, *e^+e^- collisions at 500 GeV: The Physics Potential*, Munich–Annecy–Hamburg, DESY 92–123A.

Figure Captions

- Fig. 1:** Main mechanisms for the double production of the light MSSM Higgs boson in e^+e^- collisions: a) $e^+e^- \rightarrow ZH$, $e^+e^- \rightarrow AH$ and $WW \rightarrow H$ followed by $H \rightarrow hh$; (b) $e^+e^- \rightarrow hhZ$, (c) $e^+e^- \rightarrow hhA$ and (d) $WW \rightarrow hh$.
- Fig. 2:** The cross sections for the production of the heavy CP-even Higgs boson H in e^+e^- collisions, $e^+e^- \rightarrow ZH/AH$ and $e^+e^- \rightarrow H\nu_e\bar{\nu}_e$, and for the background process $e^+e^- \rightarrow Ah$ [the dashed curve shows $\frac{1}{2} \times \sigma(Ah)$ for clarity of the figures]. The c.m. energies are chosen $\sqrt{s} = 500$ GeV in (a), and 1.5 TeV in (b).
- Fig. 3:** The branching ratios of the main decays modes of the heavy CP-even neutral Higgs boson H in (a), and of the pseudoscalar Higgs boson A in (b).
- Fig. 4:** The cross sections for hh production in the continuum for $\tan\beta = 1.5$: $e^+e^- \rightarrow hhZ$ at a c.m. energy of $\sqrt{s} = 500$ GeV (a) and $W_L W_L \rightarrow hh$ at $\sqrt{s} = 1.5$ TeV (b).
- Fig. 5:** The areas of the $[M_A, \tan\beta]$ plane in which the Higgs self-couplings λ_{Hhh} and λ_{hhh} could eventually be accessible by experiment at $\sqrt{s} = 1.5$ TeV [see text for further discussions].

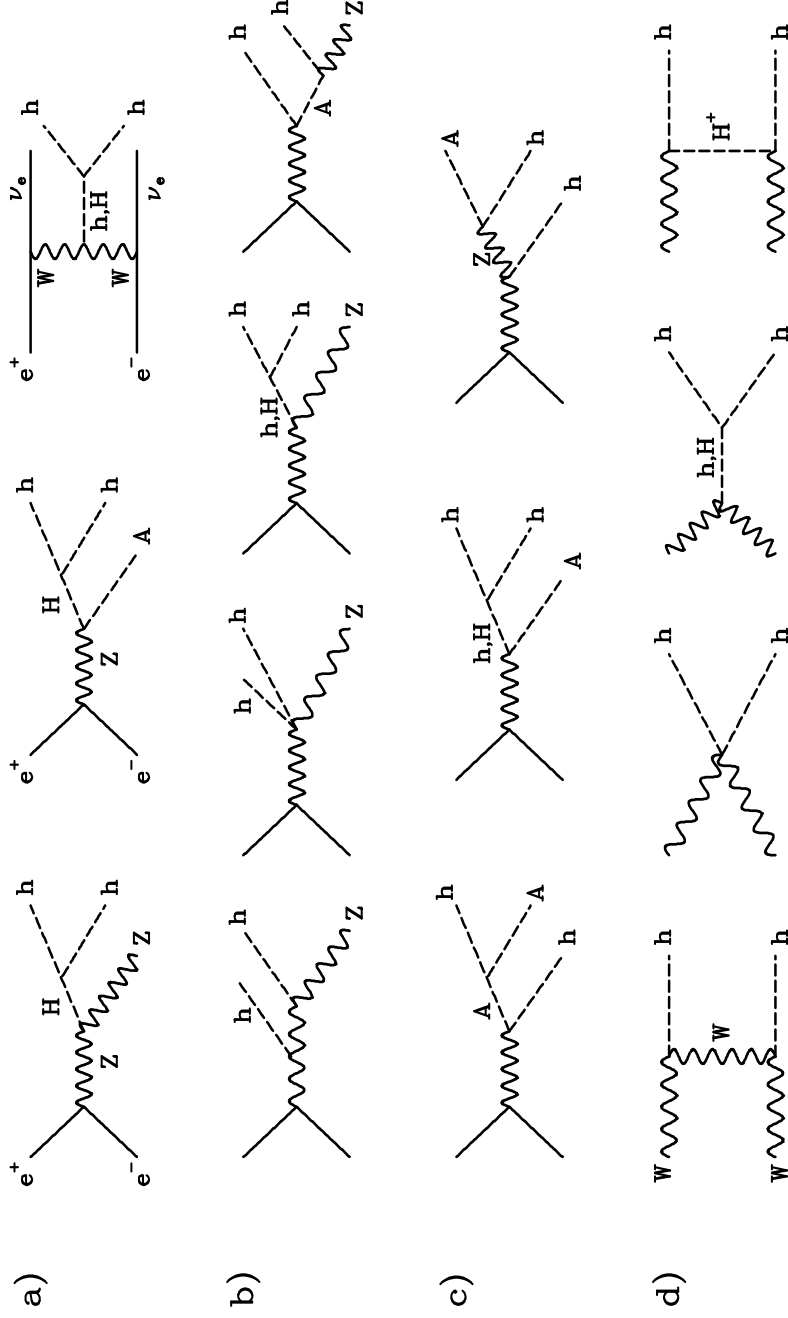


Fig. 1

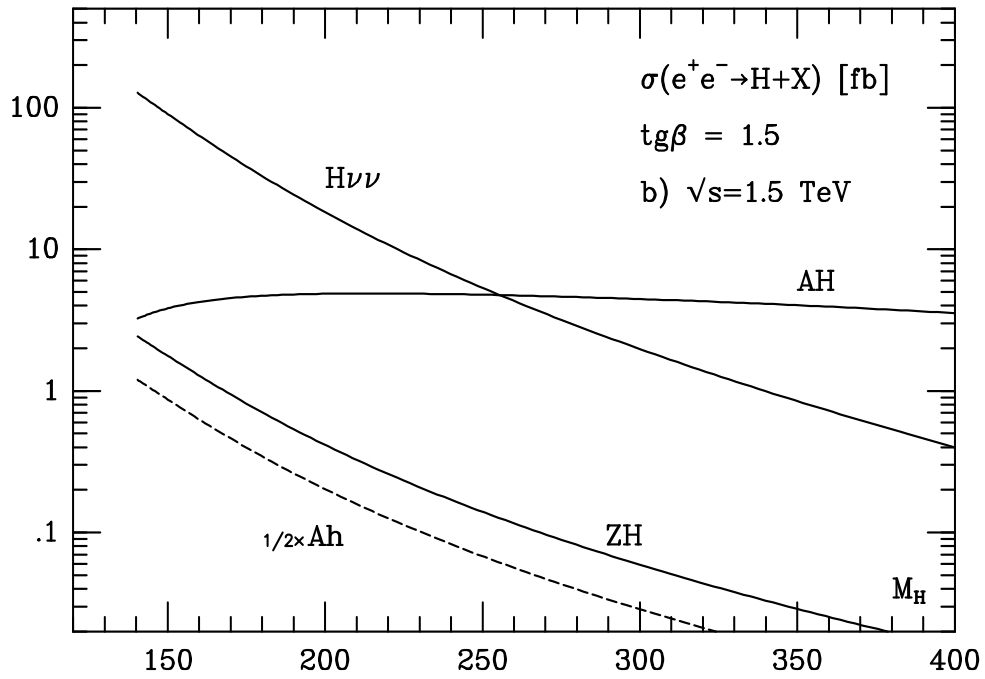
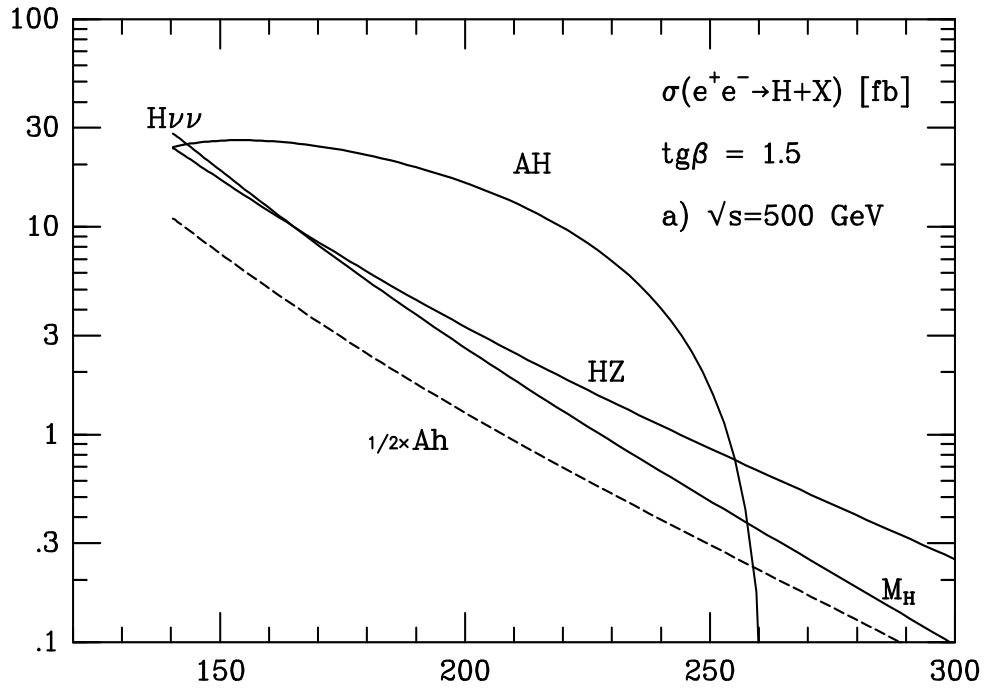


Fig. 2

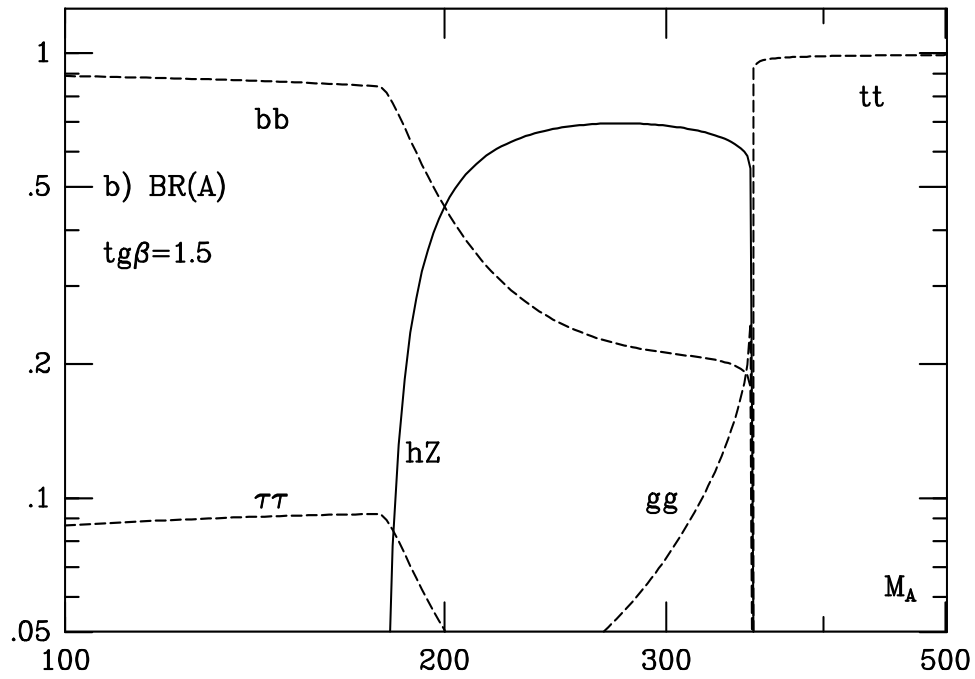
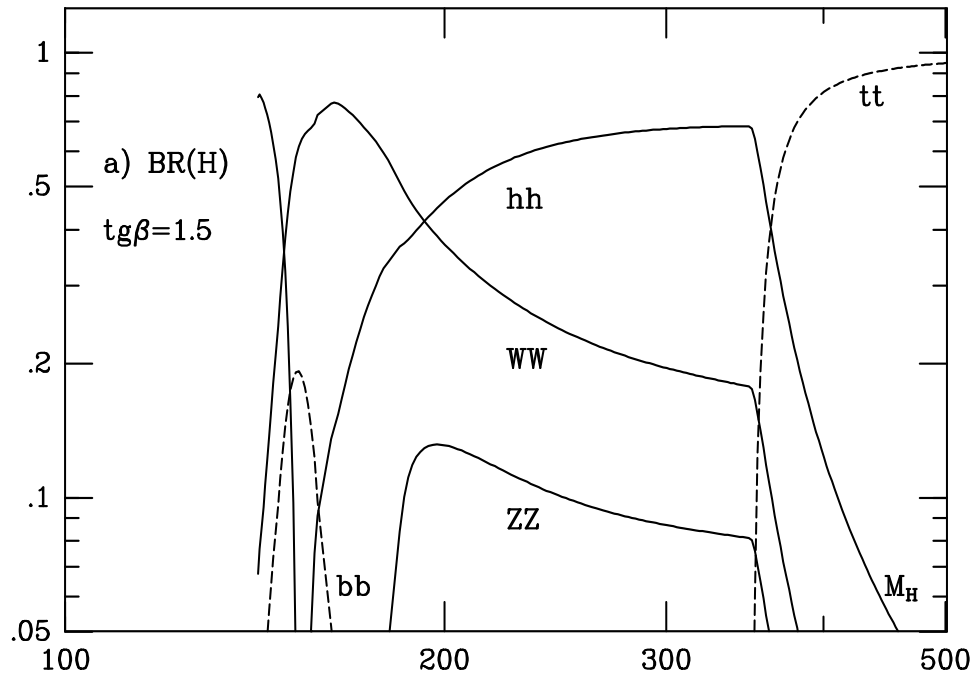


Fig. 3

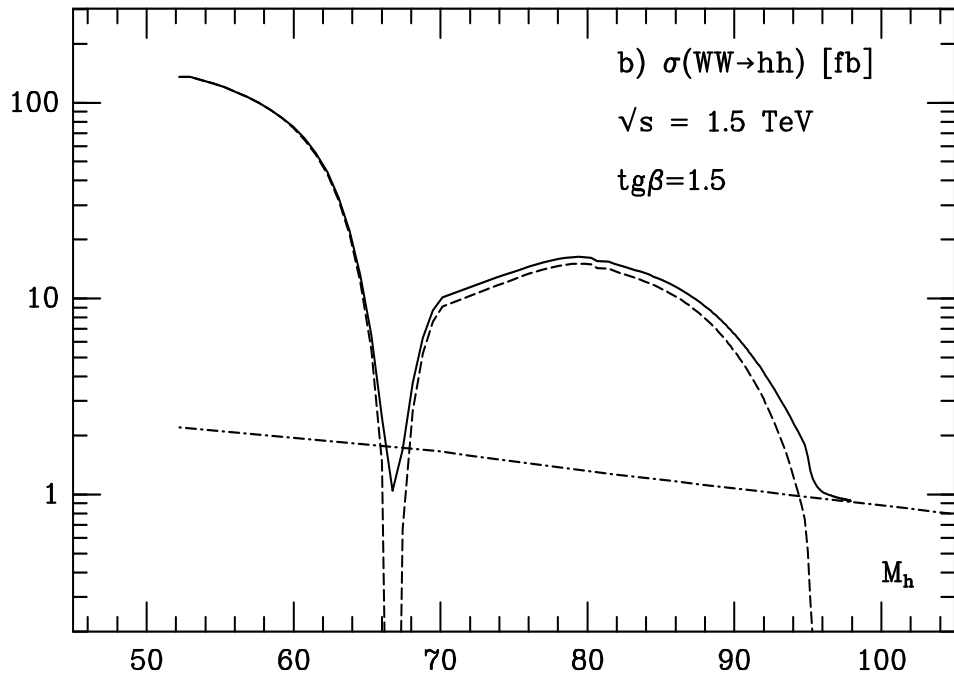
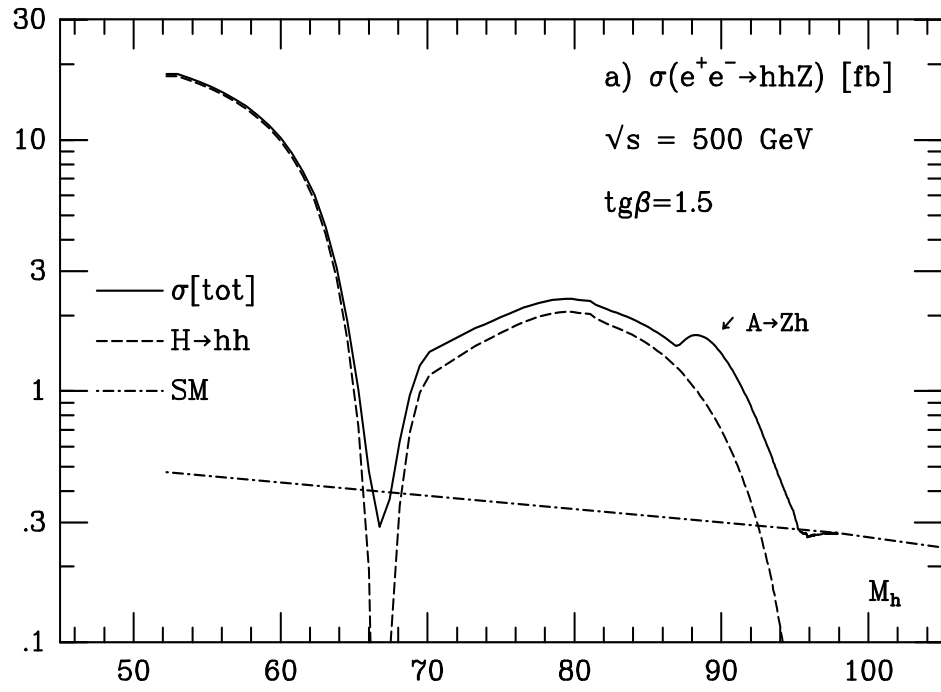


Fig. 4

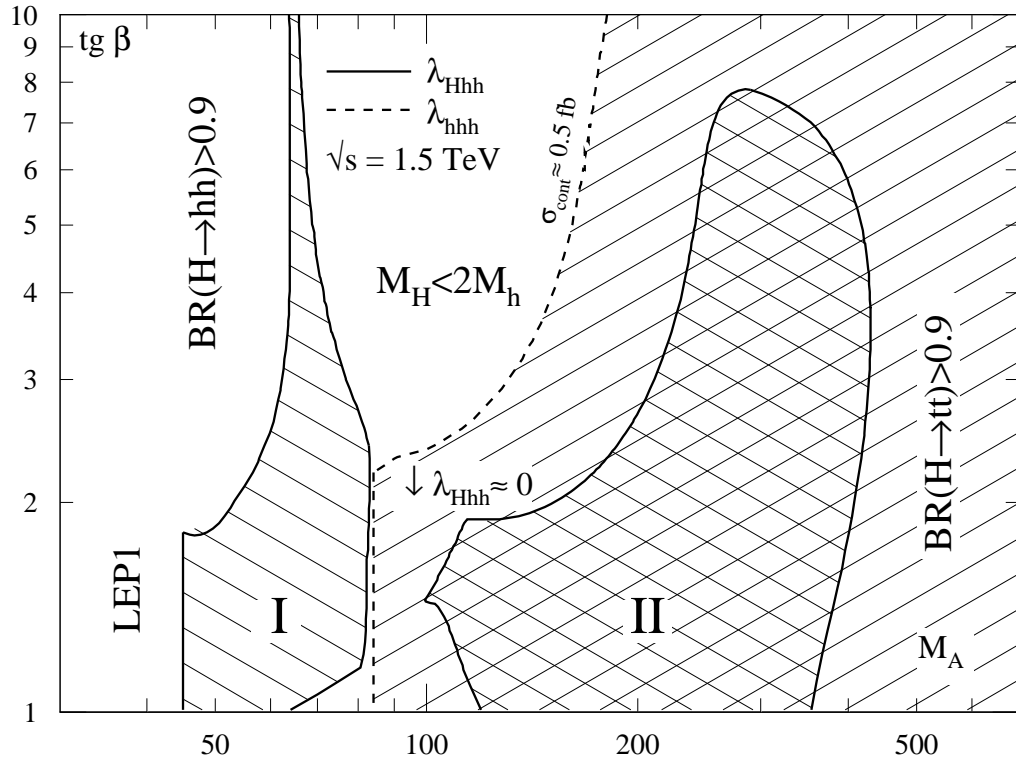


Fig. 5